Journal of Hazardous Materials 161 (2009) 336–343

Contents lists available at ScienceDirect

Journal of Hazardous Materials

journal homepage: www.elsevier.com/locate/jhazmat

Photocatalytic degradation of aqueous propoxur solution using TiO_2 and Hβ zeolite-supported TiO_2

M. Mahalakshmi, S. Vishnu Priya, Banumathi Arabindoo, M. Palanichamy, V. Murugesan*

Department of Chemistry, Anna University, Chennai 600025, India

ARTICLE INFO

Article history:
Received 30 August 2007
Received in revised form 21 March 2008
Accepted 24 March 2008
Available online 29 March 2008

Keywords:
Propoxur
Mineralization
TiO_2
Support
Hβ zeolite
TiO_2/Hβ

ABSTRACT

Photocatalytic activity of TiO_2 and zeolites supported TiO_2 were investigated using propoxur as a model pollutant. Hβ, HY and H-ZSM-5 zeolites were examined as supports for TiO_2. Hβ was chosen as the TiO_2 support based on the adsorption capacity of propoxur on these zeolites (Hβ > HY = H-ZSM-5). TiO_2/Hβ photocatalysts with different wt.% were prepared and characterized by XRD, FT-IR and BET surface area. The progress of photocatalytic degradation of aqueous propoxur solution using TiO_2 (Degussa P-25) and TiO_2 supported on Hβ zeolite was monitored using TOC analyzer, HPLC and UV–vis spectrophotometer. The degradation of propoxur was systematically studied by varying the experimental parameters in order to achieve maximum degradation efficiency. The initial rate of degradation with TiO_2/Hβ was higher than with bare TiO_2. TOC results revealed that TiO_2 requires 600 min for complete mineralization of propoxur whereas TiO_2/Hβ requires only 480 min. TiO_2/Hβ showed enhanced photodegradation due to its high adsorption capacity on which the pollutant molecules are pooled closely and hence degraded effectively.

1. Introduction

Semiconducting materials mediated photocatalytic degradation is a successful and convenient alternative to the conventional methods for the treatment of wastewater containing organic pollutants. The anatase form of TiO_2 exhibits extensive applications in the degradation of various organic pollutants [1–4]. The degradation of pollutants takes place via formation of partially oxidized intermediates, which then undergo complete mineralization. Since the reactions predominantly occur on the surface, TiO_2 supported on good adsorbents draw much attention due to three potential advantages, viz., concentration of pollutant near the TiO_2 particles, adsorption of intermediates formed and recyclability of adsorbents [5]. Among the various supports, zeolites are considered to be important owing to their special features such as high surface area, hydrophobic and hydrophilic properties, easily tunable chemical properties, high thermal stability and eco-friendly nature [6]. Zeolite-supported TiO_2 has been employed as a catalyst in photoreactions that have been performed previously on bulk powder TiO_2 [7,8]. Since TiO_2 has polar surface, it is not a good adsorbent for non-polar organic molecules [9]. Reddy et al. [10] reported the photocatalytic degradation of salicylic acid using TiO_2/Hβ zeolite. TiO_2 is well dispersed over Hβ zeolite at moderate loading which avoids particles aggregation and light scattering. The fine dispersion of TiO_2 on Hβ leaves more number of active sites near the adsorbed propoxur molecules, which result fast degradation. Further, the strong electric field present in the zeolitic framework can effectively separate the electrons and holes produced during photo excitation of TiO_2. Sankararaman et al. reported the ability of zeolites favouring photoinduced electron transfer reactions and retarding undesired back electron transfer [11]. They found that Hβ zeolite increased the adsorption of pollutants and generated large amount of hydroxyl (•OH) and peroxide radicals ($H\dot{O}_2$), which are critical species in the photocatalytic degradation process. Zeolites can delocalize excited electrons of TiO_2 and minimize e^-/h^+ recombination. TiO_2/zeolite shows enhanced photodegradation due to its high adsorption property by which the pollutant molecules are pooled closely and degraded effectively [12].

Propoxur (2-(1-methylethoxy)phenylmethyl carbamate), one of the most important *N*-methylcarbamate pesticides, is widely used in controlling numerous species of household and public health pests [13]. The long persistence of propoxur in water and its transformation products are potential contaminants in aquatic environment and food resources. In addition to its pesticidal properties, other biological effects are also reported in the literature [14,15]. It is an active acetylcholinesterase inhibitor, leading to increase acetylcholine at nerve terminals and cause symptoms such as weakness and paralysis. Due to its massive use in agricultural sector, it is increasingly detected in soil surface and wastewater. Hence it is essential to remove propoxur and its transformation prod-

* Corresponding author. Tel.: +91 44 22203144; fax: +91 44 22200660.
E-mail address: v_murugu@hotmail.com (V. Murugesan).

0304-3894/$ – see front matter © 2008 Elsevier B.V. All rights reserved.
doi:10.1016/j.jhazmat.2008.03.098

ucts from water bodies. In the present investigation, degradation of propoxur was investigated with low-pressure mercury vapour lamp of wavelengths 254 and 365 nm and compared their efficiencies. The adsorption of propoxur on Hβ was better than on HY and H-ZSM-5 and hence Hβ was selected as support in this study. Hydrophobic organic compounds such as propoxur and carbofuran showed less adsorption on zeolite supports as they are hydrophilic in nature [16]. Even though adsorption of propoxur on zeolites is low compared to 2,4-dichloroacetic acid and monocrotophos [17,18], it is expected that zeolites could enhance the degradation efficiency by delocalizing excited electrons and providing uniform diffusion of pollutant molecules towards TiO_2 surface. The degradation efficiency of TiO_2/Hβ was compared with pristine TiO_2.

2. Experimental

2.1. Materials

The commercially available TiO_2 (Degussa P-25 with 70% anatase and 30% rutile, surface area 50 m^2/g and particle size 25 nm) obtained from Degussa Chemical, Germany, was used as such. The technical grade sample of propoxur was received from Sree Ramcides Chemicals, Chennai, India. Zeolites Y, β and ZSM-5 with Si/Al ratio 3, 15 and 53, respectively purchased from Sud-Chemie India Pvt. Ltd., Mumbai, India were used as supports. All other reagents were of analytical grade and used without further purification.

2.2. Preparation of supported catalysts

Zeolite-supported TiO_2 was prepared by the method reported recently [17]. Sodium form of zeolites Y, β and ZSM-5 with Si/Al ratio 3, 15 and 53, respectively were converted into H-form by ion-exchange with 1 M ammonium nitrate solution for 24 h at 80 °C (repeated three times) with subsequent calcination at 550 °C in air for 6 h. TiO_2/Hβ with different wt.% of TiO_2 were prepared by taking appropriate amount of TiO_2 and 1 g of Hβ in acetone. This was magnetically stirred for 8 h at ambient temperature. The mixture was then filtered, dried at 110 °C for 3 h and calcined in air at 550 °C for 6 h. The prepared zeolite-supported TiO_2 materials were stored in a desiccator to prevent moisture adsorption.

2.3. Characterization of supported TiO_2

The powder XRD diffraction patterns of the materials were collected on a PANalytical X'pert PRO diffractometer equipped with Cu Kα (1.54 Å) as the radiation source and a liquid nitrogen cooled germanium solid-state detector. The samples were scanned in the 2θ range 8–80° in steps of 0.02° with a count time of 10 s at each point. The crystallinity of supported photocatalysts was calculated on relative basis by comparing the area under the characteristic peak of the parent zeolite and that of TiO_2-supported zeolite. FT-IR spectra were recorded on a FT-IR spectrometer (Nicolet Avatar 360). KBr and supported catalysts were mixed in the ratio 20:1. The mixture was ground well and made into pellets by using a hydraulic press. Such pellets were used for recording FT-IR spectra. Specific surface area was determined by the Brunauer–Emmet–Teller (BET) method using a Quantachrome Autosorb 1 sorption analyzer. Prior to adsorption of nitrogen at 77 K, the materials were degassed at 250 °C under 10^{-5} mbar pressure for 3 h.

2.4. Adsorption study

The extent of adsorption of propoxur on catalyst surface was studied by mixing 100 ml aqueous propoxur solution (200 mg l^{-1}) with 100 mg of the catalyst before the degradation process. Aliquots were withdrawn at specific time intervals and the change in propoxur concentration was measured using HPLC. The extent of adsorption was determined from the decrease in propoxur concentration. The percentage of propoxur adsorbed on the catalyst surface was calculated using the following equation:

$$\% \text{ adsorption} = \frac{C_0 - C_t}{C_0} \times 100 \quad (1)$$

where C_0 is the initial concentration of propoxur and C_t is the concentration of propoxur at time t.

2.5. Photocatalytic degradation procedure and analytical methods

Photocatalytic degradation of propoxur was performed in aqueous medium in a slurry batch reactor. A cylindrical photochemical reactor of 30 cm × 2 cm (height × diameter), provided with water circulation arrangement to maintain the temperature in the range 25–30 °C, was used in all the experiments. The irradiation was carried out using 8× 8 W low-pressure mercury lamps built into a lamp housing with polished anodized aluminium reflectors placed 12 cm away from the reactor. The lamps emit predominantly UV radiation at a wavelength of 254 nm. The other eight lamps were arranged alternatively to emit UV radiation at a wavelength of 365 nm. The reactor set-up was covered with aluminium foil followed by a black cloth to prevent UV light leakage. A stock solution containing 300 mg l^{-1} propoxur was prepared in double distilled water and diluted to the required concentrations (50–250 mg l^{-1}). TiO_2 (100 mg) was added to 100 ml propoxur solution of 200 mg l^{-1} and the resultant slurry was stirred for 30 min to attain equilibrium. It was then irradiated with UV light of either 254 or 365 nm with continuous purging of air free from CO_2. Aliquots were withdrawn at specific time intervals and analysed after centrifugation followed by filtration with 0.2 μm membrane to remove titania particles. The change in the concentration of propoxur was observed from its characteristic absorption band using a UV–vis spectrophotometer (Shimadzu 1601). The extent of degradation and formation of intermediates were followed using high performance liquid chromatograph (HPLC) (Shimadzu, LC-10 ATvp pump and SPD-10Avp UV–vis detector adjustable to 210 and 270 nm with reverse phase ODS column). The mobile phase was composed of acetonitrile and triple distilled water (60:40, v/v). The extent of mineralization of propoxur was measured using total organic carbon analyzer (Shimadzu TOC-V CPN). The formation of NO_3^- ions was identified and confirmed by injecting a blank solution of sodium nitrate in HPLC. The formation of NH_4^+ ions was confirmed by the addition of Nessler's reagent to the aqueous solution.

3. Results and discussion

3.1. Physico-chemical characterization of photocatalysts

The XRD patterns of Hβ, TiO_2 and Hβ supported TiO_2 catalysts are shown in Fig. 1. The XRD peaks of crystal phase [1 0 1] for anatase appeared at 25.4° (2θ) and the crystal phase [1 1 0] for rutile appeared at 27.5° (2θ) [16]. The representative peaks at 25.8° and 22.4° (2θ) corresponding to Hβ are in good agreement with the previous reports [18]. The gradual increase in the intensity of TiO_2 peak at 25.4° (2θ) and consequent decrease in the intensity of representative peaks of Hβ clearly illustrate that there is false scattering of diffracted rays of Hβ/TiO_2 grains on the zeolite surface. The mid-FT-IR spectrum of Hβ zeolite is shown in Fig. 2 (spectrum a). The broad band between 2500 and 3800 cm^{-1} is due to –OH stretching of defective SiOH groups, water and Si–O–Al bridges of

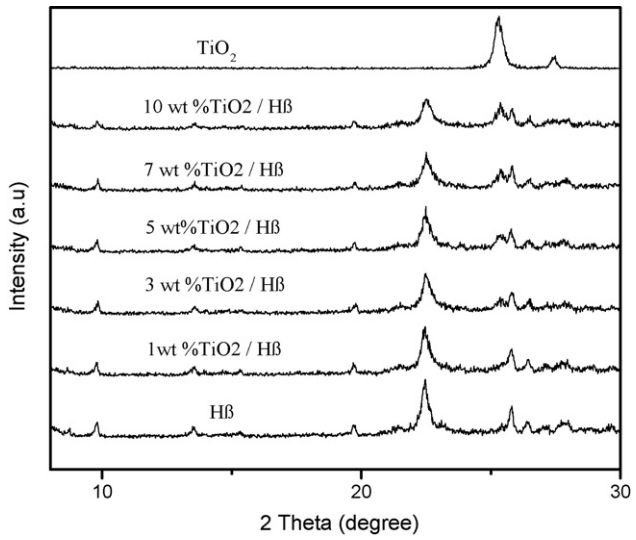

Fig. 1. XRD patterns of Hβ, TiO_2/Hβ and TiO_2.

zeolites. The bending mode of water is observed at 1636 cm^{-1}. The framework asymmetric vibrations of Si–O–Si and Si–O–Al give an intense broad band between 1500 and 850 cm^{-1} and the symmetric vibration at 797 cm^{-1}. The peak below 700 cm^{-1} is due to framework bending modes. The mid-FT-IR spectrum of TiO_2 is also shown in Fig. 2 (spectrum g). The intense broad band below 1200 cm^{-1} is due to Ti–O vibration. The spectra b–f shown in the same figure correspond to 1, 3, 5, 7 and 10 wt.% TiO_2/Hβ catalysts. Though the spectra appear similar, there are still some variations in the region of the bending modes of Hβ framework. The symmetric vibration of Si–O–Si (797 cm^{-1}) is clearly resolved in the spectrum of Hβ (spectrum a) but its intensity decreases with increase in TiO_2 loading up to 10 wt.%. This is attributed to intense Ti–O stretching overlapped with Si–O–Si vibration. The intensity of $O–H_2$ bending mode increases up to 5 wt.% but decreases for 7 and 10 wt.% TiO_2/Hβ. There may be transfer of outer surface Bronsted acid sites of Hβ to TiO_2 particles up to 5 wt.% TiO_2 loading. Hence both negatively charged Si–O–Al bridge and protonated TiO_2 particles could adsorb water. But the excess TiO_2 particles block the acid sites in 7 and 10 wt.% TiO_2/Hβ. Hence the intensity of OH_2 bending mode decreases for higher loading of TiO_2/Hβ. The O–H stretching vibration in the high-energy region also shows such variation with increase in TiO_2 loading.

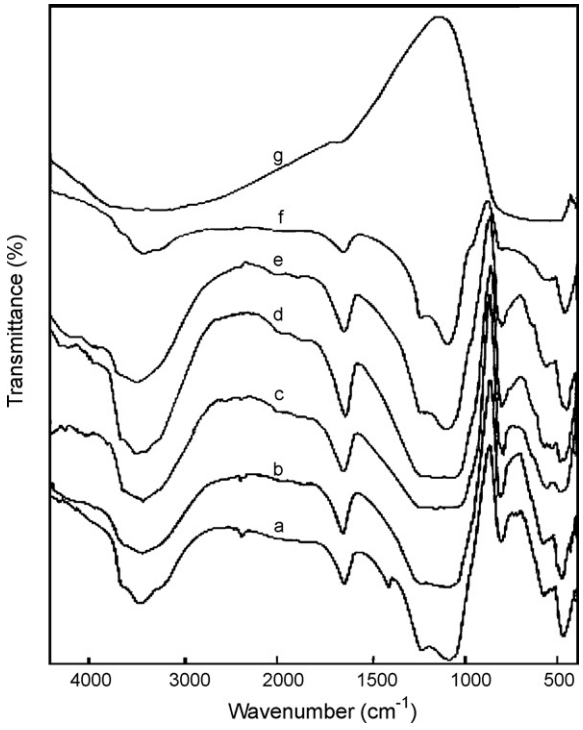

Fig. 2. FT-IR spectra of (a) Hβ, (b) 1 wt.% TiO_2/Hβ, (c) 3 wt.% TiO_2/Hβ, (d) 5 wt.% TiO_2/Hβ, (e) 7 wt.% TiO_2/Hβ, (f) 10 wt.% TiO_2/Hβ and (g) TiO_2.

Table 1
Surface area of the catalysts

Catalyst	Surface area (m^2 g^{-1})
TiO_2	50
Hβ	575
Amount of TiO_2 (g) per gram of Hβ	
0.01	545
0.03	522
0.05	499
0.07	425

The BET surface area of TiO_2, Hβ and TiO_2/Hβ are presented in Table 1. The surface area of the supported photocatalysts decreases with increase in the loading of TiO_2. This is possibly due to aggregation of TiO_2 particles on the surface and blocking of the pores of Hβ [17].

3.2. Adsorption

The results indicate that propoxur is better adsorbed over Hβ than HY and H-ZSM-5 (Table 2). The low adsorption capability of HY and H-ZSM-5 is attributed to hydrophilic nature of HY and low surface area of H-ZSM-5 (BET surface area of the catalysts: HY = 648 m^2/g, Hβ = 575 m^2/g and H-ZSM-5 = 386 m^2/g). Apart from hydrophilicity and surface area, the presence of acid sites with good acid strength in Hβ could also be yet another reason for better adsorption of propoxur. The presence of –NH group in the carbamate pesticide enhanced the adsorption on less hydrophilic surface. Hence, Hβ was chosen as the support in this study. It is also expected that zeolites could enhance the degradation efficiency by delocalising excited electrons and providing uniform diffusion of pollutant molecules towards TiO_2 surface.

3.3. Photocatalytic degradation of propoxur

The effect of reaction variables such as pH of the solution, initial concentration of propoxur, catalyst loading and light intensity on the rate of degradation was studied and the results are delineated below.

3.3.1. Effect of pH

The solution pH is an important variable in aqueous phase mediated photocatalytic reactions. The pH of a solution influ-

Table 2
Adsorption capacity of zeolites, TiO_2 (Degussa P-25) and Hβ supported TiO_2

Pesticide	Propoxur
Adsorption (mmol/g)	
Hβ	25
HY	2.3
H-ZSM-5	2.3
TiO_2	5.5
TiO_2/Hβ (7 wt.%)	20

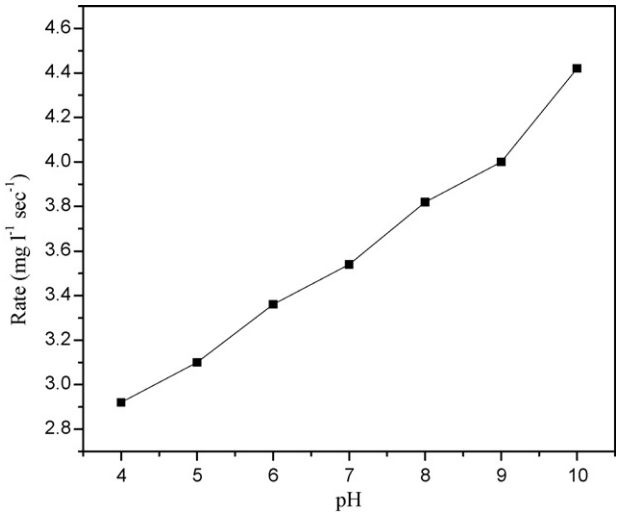

Fig. 3. Effect of pH on the rate of degradation.

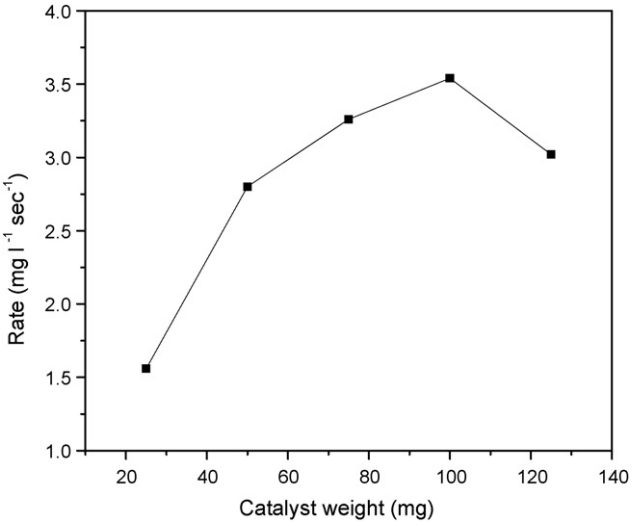

Fig. 5. Effect of catalyst loading on the rate of degradation.

ences adsorption and dissociation of substrate, catalyst surface charge, oxidation potential of the valence band and other physicochemical properties of the system [19]. The effect of pH on the rate of photocatalytic degradation was studied by keeping all other experimental conditions constant and varying the initial pH of the propoxur solution from 4 to 10. The results are depicted in Fig. 3. The rate of degradation increases with increase in pH from 4 to 10. The hydrolysis of propoxur was found to be good under alkaline condition [13]. The propoxur undergoes significant hydrolysis in water above pH 8 and hence its degradation is high in the alkaline pH.

3.3.2. *Effect of initial concentration of propoxur*

The effect of initial concentration of propoxur on the overall rate of degradation was studied by varying the initial concentration from 50 to 250 mg l^{-1}. The results are depicted in Fig. 4. The rate of degradation increases with increase in the propoxur concentration up to 200 mg l^{-1}. But above this concentration the rate decreases due to insufficient quantity of •OH radicals, as the formation of •OH radicals is a constant for a given amount of the catalyst. The generation of •OH radicals may also be reduced at higher propoxur concentration since the precursor (OH^- ions) of •OH radicals are replaced by 2-isopropoxyphenolic anions which are produced by the degradation and hydrolysis of propoxur [15].

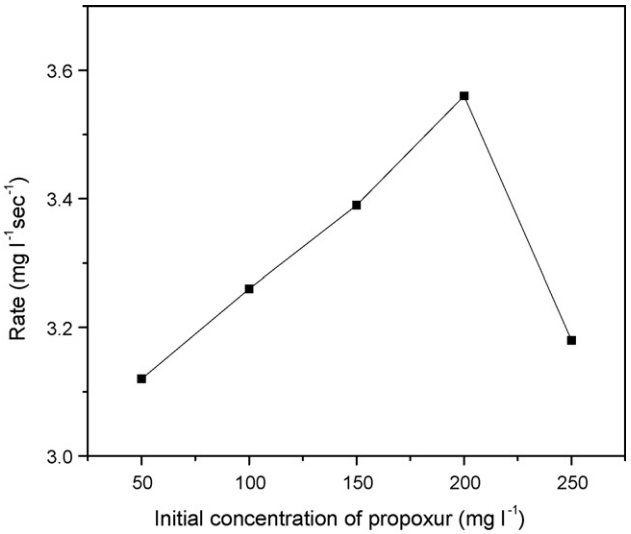

Fig. 4. Effect of initial concentration on the rate of degradation.

$$\text{Propoxur} \rightarrow \text{2-isopropoxyphenol} + \text{formamide} \quad (2)$$

At higher concentrations, the screening effect also dominates [18,20,21] and hence degradation efficiency decreases.

3.3.3. *Effect of catalyst loading*

The effect of catalyst loading on the rate of degradation of propoxur was investigated keeping all other experimental parameters constant and the results are shown in Fig. 5. There is a steady increase in the rate of degradation up to 100 mg of the catalyst beyond which the rate decreases. The increase of catalyst loading from 25 to 100 mg increases the degradation rate due to increase in the catalyst surface area, which enhances absorption of photons. The decrease at higher loading beyond the optimum level of 100 mg is due to decrease in the light penetration and deactivation of activated molecules due to collision with the ground state molecules [18]. Further, at higher catalyst loading it is difficult to maintain the suspension homogeneous due to particles agglomeration which decreases the number of active sites [22].

3.3.4. *Effect of light intensity*

The effect of light intensity was investigated under the optimized experimental conditions using 2, 4, 6 and 8 UV lamps of 254 nm, each with 8 W power (electric power consumed) corresponding to light intensity of 354, 600, 796 and 896 lux unit, respectively as calculated from lux meter (Model nv-light meter Lx-101A X1 Lux). The results are illustrated in Fig. 6. The rate of degradation increases with increase in light intensity up to eight lamps corresponding to 64 W of light intensity 896 lux. This demonstrates that the rate of degradation is directly proportional to light intensity [23]. When the intensity of incident light increases, the probability of excitation of electrons also increases and hence increases the degradation rate.

3.3.5. *Mineralization of propoxur*

The extent of degradation and mineralization was followed using HPLC and TOC analyzer, respectively. The HPLC chromatograms reveal the degradation of propoxur into small fragments, which are subsequently mineralized completely. The mineralization of propoxur was studied with lamps of wavelengths 254 and 365 nm. Though the mineralization rates apparently

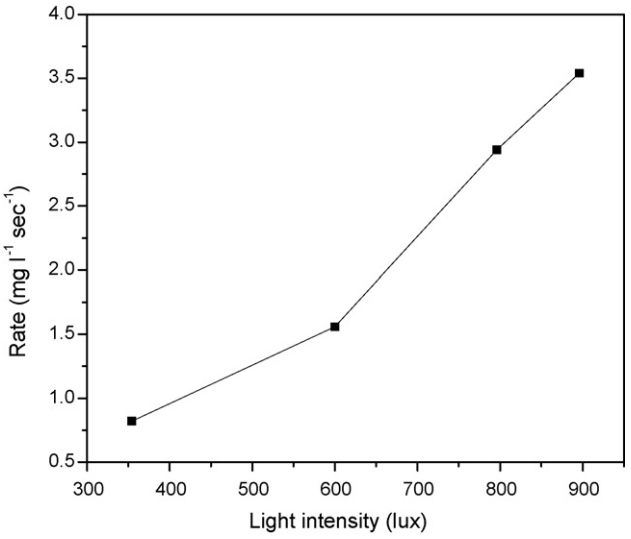

Fig. 6. Effect of light intensity on the rate of degradation.

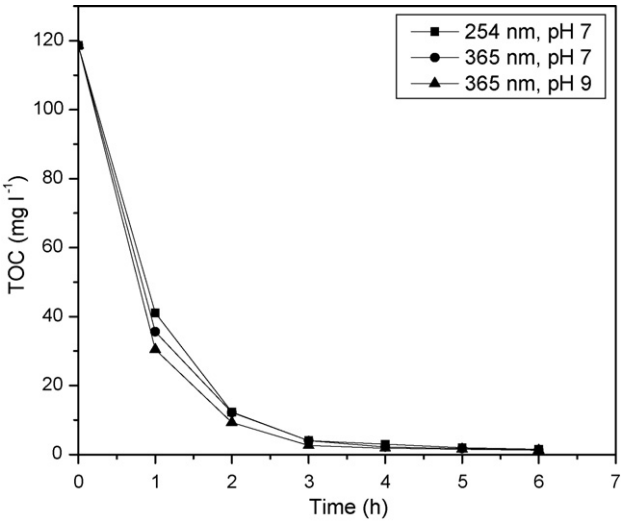

Fig. 8. Effect of irradiation time on the mineralization of propoxur at 254 and 365 nm.

appear to be nearly equal for both the lamps, the mineralization rate with 365 nm is unexpectedly slightly higher than with 254 nm. This may be accounted by considering partial absorption and wasting of the light of 254 nm by propoxur itself. The UV spectrum of propoxur between 200 and 400 nm illustrates considerable absorption at 254 nm (Fig. 7). Similar result was also observed in the photocatalytic degradation of carbofuran, a carbamate pesticide in our earlier study [24]. Both the carbamate pesticides show nearly same UV–vis absorption maxima, viz., 210 and 275 nm for carbofuran and 207 and 270 nm for propoxur. Thus the entire light of irradiation at 254 nm in the reactor is not used for the excitation of TiO_2 particles because of the absorption of light by intervening propoxur molecules as well as those adsorbed on TiO_2 particles. Hence absorption and wasting of light at 254 nm by propoxur may be the actual cause for lower rate of degradation than at 365 nm. Thus it is concluded that the pollutant should possess negligible absorption close to the wavelength of irradiation source for better photocatalytic degradation. Since the lamp with wavelength of 365 nm showed higher efficiency than 254 nm (Fig. 8), the mineralization study was carried out with the lamp of 365 nm. The absorption peaks (207 and 270 nm) corresponding to propoxur showed a linear dependence with initial concentration of propoxur.

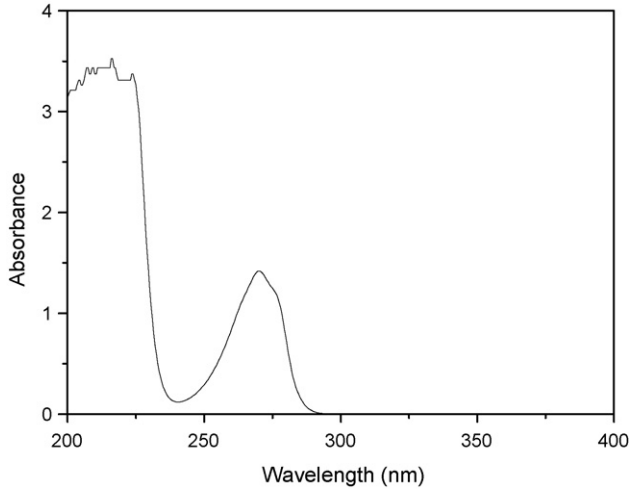

Fig. 7. UV–vis absorption spectrum of propoxur.

The complete mineralization of propoxur (200 mg l^{-1}) with 100 mg of TiO_2 using low-pressure mercury vapour lamp of 365 nm at pH 7 and 9 was achieved in 5 h (Fig. 10). Though the initial rate of degradation was higher (4.0 mg l^{-1} s^{-1}) at pH 9 than at 7 (3.54 mg l^{-1} s^{-1}), the rate of degradation was almost the same after 3 h irradiation. Though the alkaline condition initially favoured the hydrolysis of propoxur, the degradation predominated over hydrolysis with increasing irradiation time. Hence the degradation of propoxur was independent of solution pH at longer irradiation time.

Tennakone et al. [25] reported the formation of NO_3^-, NO_2^- and NH_4^+ ions in the photocatalytic mineralization of carbofuran using TiO_2. Propoxur, the similar family of *N*-methylcarbamate pesticide also produced NO_3^- and NH_4^+ ions in solution at the end of photomineralization. Since the attack of hydroxyl radicals can induce cleavage of C–N bond of the pesticide, the organic nitrogen is transferred into NO_3^-, NO_2^- and NH_4^+ ions [26,27]. The concentration of nitrate ions increased rapidly with increase in irradiation time. The peak in the HPLC chromatogram at a retention time of 1.76 min for the irradiated sample coincided with the peak for sodium nitrate solution. At the end of degradation process 1.25×10^{-4} mol l^{-1} of NO_3^- ion was produced, corresponding to ca. 48% of the initial nitrogen in propoxur. The carbamate group is the primary site of attack by the hydroxyl radical giving carbamic acid, which is a known unstable compound and hence decomposes rapidly to gaseous products such as methyl amine and carbon dioxide. Since TOC results confirmed that TiO_2 requires 300 min for complete mineralization of propoxur (Fig. 8), the incomplete mass balance of nitrogen may be accounted by the fact that certain portion of nitrogen is evolved as volatile organic compound such as methyl amine. Such incomplete mass balance has been already reported in the degradation of carbofuran [24]. During the degradation of propoxur, isopropoxyphenol and *N*-methylformamide were identified as the degradation products [13]. The formation of NH_4^+ ion in the degradation of *N*-methylformamide was identified using Nessler's reagent. However, these NH_4^+ ions eventually transformed into NO_3^- and H^+ ions [26,27].

3.3.6. Photodegradation products of propoxur

The photocatalytic degradation products formed during the degradation of propoxur were identified using GC–MS. The irradiation time was optimized in order to acquire intense peaks for intermediates in the HPLC chromatograms and then anal-

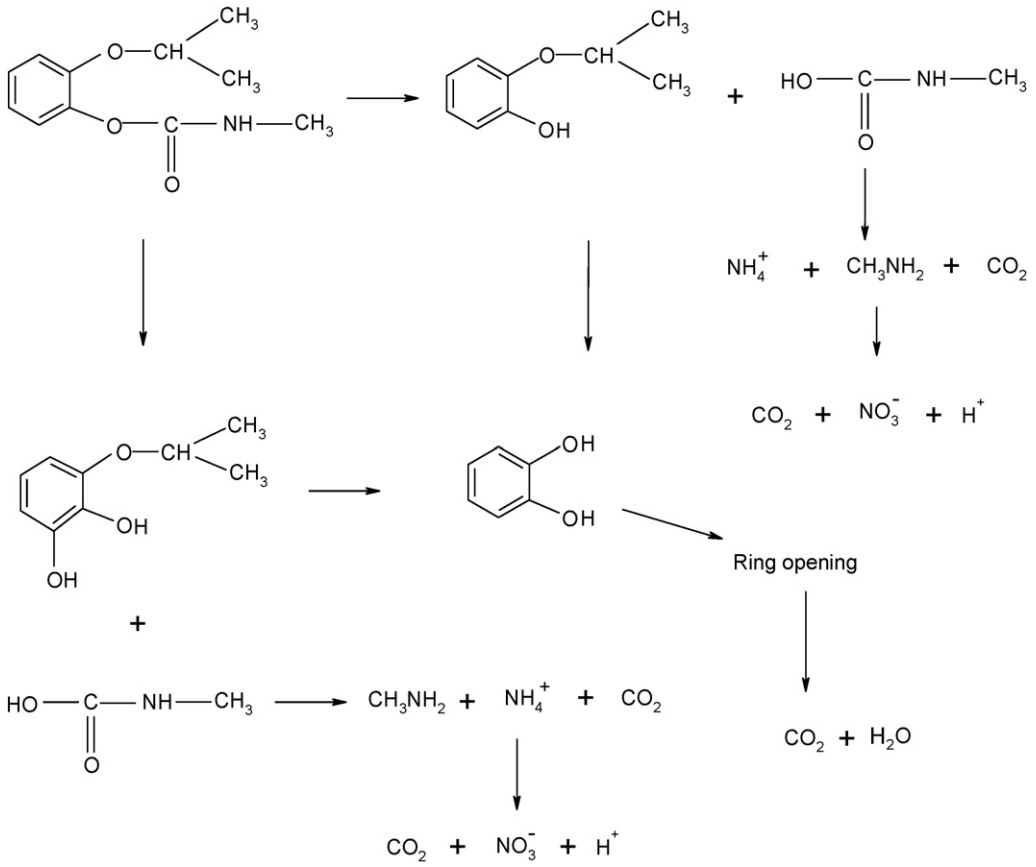

Scheme 1. Plausible pathway for the degradation of propoxur.

ysed by GC–MS for better resolution. Propoxur samples irradiated for 1 h showed very low intense peaks for intermediates and hence 30 min irradiated samples were extracted and analysed using GC–MS. The aliphatic side chains cleaved to form fragments and subsequently degraded. The products identified were 2-(1-methylethoxy)-phenol (2-isopropoxyphenol), 2-hydroxy-3-(1-methylethoxy)-phenol (2-isopropoxycatechol) and 2-hydroxy phenol (catechol). The same photocatalytic degradation products were reported by Sanjuan et al. [28]. The plausible degradation pathway based on the intermediates formed during degradation is shown in Scheme 1. The carbamate group is the primary site of attack by the hydroxyl radical resulting carbamic acid. This decomposes rapidly to give gaseous products such as methyl amine and carbon dioxide. The cleavage of benzene ring and subsequent mineralization leading to water and carbon dioxide could be visualised from the decrease in TOC during the photocatalytic process.

3.4. Effect of TiO_2 loaded on Hβ zeolite

Photocatalytic degradation of propoxur was carried out under optimized conditions with 3, 5, 7 and 10 wt.% TiO_2 loaded on Hβ in order to understand their influence in the degradation efficiency. The increase in the amount of TiO_2 on Hβ zeolite increases the extent of degradation up to 7 wt.% and then decreases (Fig. 9). At higher TiO_2 loading (>7 wt.%), the extent of degradation decreased due to less adsorption of propoxur and light scattering effect. Moreover, the excited TiO_2 particles may not be close to the zeolite surface at higher percentage loading and hence its conduction band electrons are not delocalized over zeolite. As a result the rate of electron–hole recombination could be fast and hence the degradation rate decreased. Hence an optimum loading of TiO_2 on zeolite surface alone can enhance the degradation. Since TiO_2 is polar in nature and also possesses low surface area, the adsorption of non-polar compounds is less. In the present study, the optimum loading of TiO_2 on Hβ is found to be 7 wt.%.

3.5. Degradation of propoxur on TiO_2 and TiO_2/Hβ

TiO_2/Hβ (7 wt.%) required shorter irradiation time for complete mineralization of propoxur than pristine TiO_2 due to enhanced adsorption of propoxur and its intermediates on the catalyst sur-

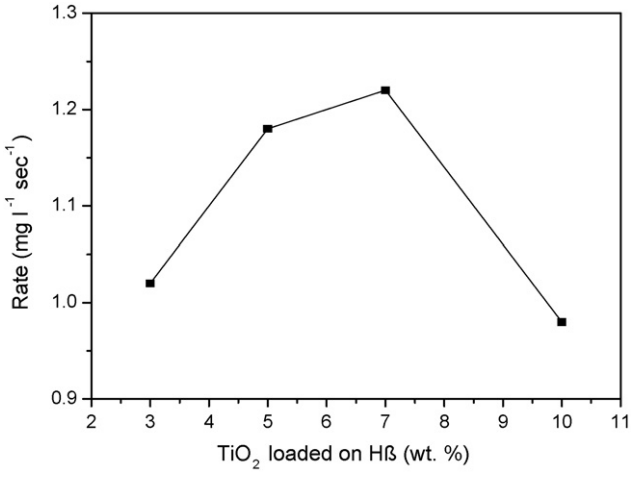

Fig. 9. Effect of TiO_2 loading on Hβ on the rate of degradation of propoxur.

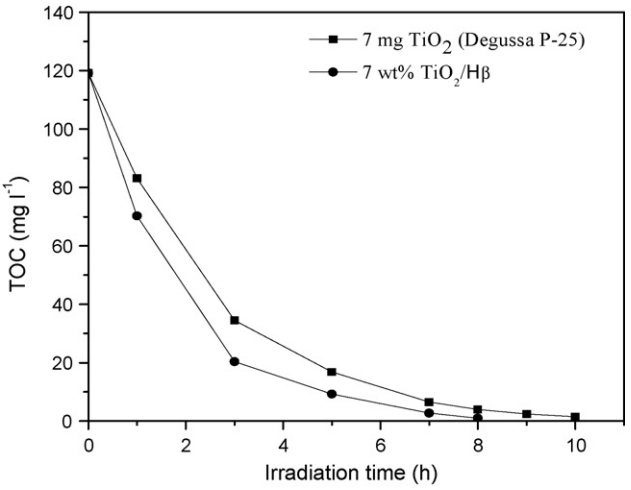

Fig. 10. The effect of irradiation time on the mineralization of propoxur over TiO_2 and TiO_2/Hβ.

face. The •OH radicals are strong enough to break different (C–C, C–N and C=O) bonds in the propoxur molecules adsorbed on the surface of TiO_2 leading to the formation of CO_2 and inorganic ions [29]. The extent of propoxur mineralization increased with increase of irradiation time. The initial rate of degradation with TiO_2/Hβ ($1.22\,mg\,l^{-1}\,s^{-1}$) is higher than pristine TiO_2 ($0.82\,mg\,l^{-1}\,s^{-1}$). The light-induced degradation followed by mineralization was much faster in the first 60 min on TiO_2/Hβ and thereafter the extent of mineralization is slow. This is due to competitive adsorption of intermediates such as isopropanol and *N*-methylformamide and the parent propoxur molecule. Further, the formation of NO_3^- ions reduced the reaction rate as they also adsorbed on the catalyst surface. Such hindering effects have already been reported in the photocatalytic degradation of textile dyes [30].

The low degradation rate is also attributed due to low reactivity of short chain aliphatic compounds such as isopropanol and *N*-methylformamide with •OH radicals [31]. The intermediates on the catalyst surface also degraded with increase in irradiation time. The mineralization of propoxur under optimal conditions revealed that propoxur could be mineralized completely in a shorter period with supported catalyst than with pure TiO_2. TOC results revealed that pure TiO_2 required 600 min for complete mineralization of propoxur whereas TiO_2/Hβ required only 480 min (Fig. 10). The higher adsorption capacity of supported TiO_2 than pure TiO_2 resulted higher propoxur concentration around TiO_2 particles, which enhanced the possibility of attack of photogenerated active species on propoxur molecules. At moderate loading, TiO_2 is well dispersed over Hβ zeolite thus preventing particles aggregation and light scattering. The fine dispersion of TiO_2 on Hβ left more number of active sites near the adsorbed propoxur molecules, which resulted fast degradation. Further, the strong electric field present in the zeolitic framework effectively separated the electrons and holes produced during photo excitation of TiO_2 [32].

4. Conclusions

Hβ zeolite is found to be better support for TiO_2 than HY and HZSM-5 based on the adsorption capacity of propoxur. The degradation efficiency of TiO_2/Hβ is higher than pristine TiO_2. The higher adsorption of propoxur on TiO_2/Hβ enhances the degradation efficiency. The hydrophilic intermediates are strongly adsorbed on the catalyst surface of TiO_2/Hβ which exhibit complete mineralization. The degradation efficiency of propoxur is higher in TiO_2/Hβ with optimum loading of TiO_2 (7 wt.%) than pure TiO_2. The TOC results demonstrate that TiO_2/Hβ required less time for total mineralization of propoxur than pure TiO_2.

Acknowledgements

The authors gratefully acknowledge the University Grants Commission (UGC), New Delhi, for liberal funding through the Centre with Potential for Excellence in Environmental Sciences (CPEES) at our University for creating necessary instrumentation facilities to carry out the research work.

References

[1] A. Fujishima, T.N. Rao, A.D. Tryk, Titanium dioxide photocatalysis, J. Photochem. Photobiol. C: Photochem. Rev. 1 (2000) 1–21.
[2] M.R. Hoffmann, S.T. Martin, W. Choi, D.W. Bahnemann, Environmental applications of semiconductor photocatalysis, Chem. Rev. 95 (1995) 69–96.
[3] M.A. Fox, M.T. Dulay, Hetereogenous photocatalysts, Chem. Rev. 93 (1993) 341–357.
[4] N. Serpone, E. Pelizzetti, in: N. Serpone, E. Pellizzetti (Eds.), Photocatalysis: Fundamentals and Applications, John Wiley and Sons, New York, 1989.
[5] J. Chen, L. Eberlein, C.H. Langford, Pathways of phenol and benzene photooxidation using TiO_2 supported on a zeolite, J. Photochem. Photobiol. A 148 (2002) 183–189.
[6] A. Corma, From microporous to mesoporous molecular sieve materials and their use in catalysis, Chem. Rev. 97 (1997) 2373–2420.
[7] H. Yoneyama, T. Torimoto, Titanium dioxide/adsorbent hybrid photocatalysts for photodestruction of organic substances of dilute concentrations, Catal. Today 58 (2000) 133–140.
[8] T. Torimoto, S. Ito, S. Kuwabata, H. Yoneyama, Effects of adsorbents used as supports for titanium dioxide loading on photocatalytic degradation of propyzamide, Environ. Sci. Technol. 30 (1996) 1275–1281.
[9] Y. Xu, C.H. Langford, Enhanced photoactivity of titanium (IV) oxide supported on ZSM-5 and zeolite at low coverage, J. Phys. Chem. 99 (1995) 11501–11507.
[10] E.P. Reddy, L. Davydov, P. Smirniotis, TiO_2-loaded zeolites and mesoporous materials in the sonophotocatalytic decomposition of aqueous organic pollutants: the role of the support, Appl. Catal. B: Environ. 42 (2003) 1–11.
[11] S. Sankararaman, K.B. Yoon, T. Yabe, J.K. Kochi, Control of back electron transfer from charge-transfer ion pairs by zeolite supercages, J. Am. Chem. Soc. 113 (1991) 1419–1421.
[12] M. Noorjahan, V.D. Kumari, M. Subrahmanyam, P. Boule, A novel and efficient photocatalyst: TiO_2–H-ZSM-5 combinate thin film, Appl. Catal. B: Environ. 47 (2004) 209–213.
[13] L. Sun, H.K. Lee, Stability studies of propoxur herbicide in environmental water samples by liquid chromatography–atmospheric pressure chemical ionization ion-trap mass spectrometry, J. Chromatogr. A 1014 (2003) 153–163.
[14] C.W. Stanley, J.S. Thorton, Gas-chromatographic method for residues of Baygon and its major metabolite in animal tissues and milk, J. Agric. Food Chem. 20 (1972) 1269–1273.
[15] M. Guardia de la, K.D. Khalaf, V. Carbonell, A.M. Rubio, Clean analytical method for the determination of propoxur, Anal. Chim. Acta 308 (1995) 462–468.
[16] Y.H. Hsien, C.F. Chang, Y.H. Chen, S. Cheng, Photodegradation of aromatic pollutants in water over TiO_2 supported on molecular sieves, Appl. Catal. B: Environ. 31 (2001) 241–249.
[17] M.V. Shankar, S. Anandan, N. Venkatachalam, B. Arabindoo, V. Murugesan, Fine route for an efficient removal of 2,4-dichlorophenoxyacetic acid (2,4-D) by zeolite supported TiO_2, Chemosphere 63 (2006) 1014–1021.
[18] M.V. Shankar, K.K. Cheralathan, B. Arabindoo, M. Palanichamy, V. Murugesan, Enhanced photocatalytic activity for the destruction of monocrotophos pesticide by TiO_2/Hβ, J. Mol. Catal. 223 (2004) 195–200.
[19] M.V. Shankar, S. Anandan, N. Venkatachalam, B. Arabindoo, V. Murugesan, Novel thin-film reactor for photocatalytic degradation of pesticides in aqueous solutions, J. Chem. Technol. Biotechnol. 79 (2004) 1279–1285.
[20] B. Neppolian, S. Sakthivel, M. Palanichamy, B. Arabindoo, V. Murugesan, Photoassisted degradation of textile dye using ZnO catalyst, Bull. Catal. Soc. India 9 (1999) 164–171.
[21] S. Sakthivel, B. Neppolian, M.V. Shankar, B. Arabindoo, M. Palanichamy, V. Murugesan, Solar photocatalytic degradation of azo dye: comparison of photocatalytic efficiency of ZnO and TiO_2, Solar Energy Mater. Solar Cells 77 (2003) 65–82.
[22] S. Rabindranathan, D.P. Suja, S. Yesodharan, Photocatalytic degradation of phosphamidon on semiconductor oxides, J. Hazard. Mater. B 102 (2003) 217–229.
[23] K. Mehrotra, G.S. Yablonsky, A.K. Ray, Kinetic studies of photocatalytic degradation in a TiO_2 slurry system: Distinguishing working regimes and determining rate dependences, Ind. Eng. Chem. Res. 42 (2003) 2273–2281.
[24] M. Mahalakshmi, B. Arabindoo, M. Palanichamy, V. Murugesan, Photocatalytic degradation of carbofuran using semiconductor oxides, J. Hazard. Mater. 143 (2007) 240–245.

[25] K. Tennakone, C.T.K. Tilakaratne, I.R.M. Kottegoda, Photomineralization of carbofuran by TiO_2-supported catalyst, Water Res. 31 (1997) 1909–1912.
[26] M. Klare, J. Scheen, K. Vogelsang, H. Jacobs, J.A.C. Broekaert, Degradation of short-chain alkyl- and alkanolamines by TiO_2- and Pt/TiO_2-assisted photocatalysis, Chemosphere 41 (2000) 353–362.
[27] K. Waki, J. Zhao, S. Horikoshi, N. Watanabe, H. Hidaka, Photooxidation mechanism of nitrogen-containing compounds at TiO_2/H_2O interfaces: an experimental and theoretical examination of hydrazine derivatives, Chemosphere 41 (2000) 337–343.
[28] A. Sanjuan, G. Aguirre, M. Alvaro, H. Garcia, J.C. Scaiano, Degradation of propoxur in water using 2,4,6-triphenylpyrylium–zeolite Y as photocatalyst, Appl. Catal. B: Environ. 25 (2000) 257–265.
[29] J. Gimenez, M.A. Aguado, S. Cervera, L. Borrell, D. Lurco, M.A. Queral, in: D.E. Klett, R.E. Hogon, T. Tanaka (Eds.), Solar Engineering, The American Society of Mechanical Engineers, New York, 1994, pp. 291–297.
[30] M.V. Shankar, B. Neppolian, B. Arabindoo, M. Palanichamy, V. Murugesan, Kinetics of photocatalytic degradegradation of textile dye reactive red 2, Ind. J. Eng. Mater. Sci. 8 (2001) 104–109.
[31] C.A. Martin, M.A. Baltanas, A.E. Cassano, Photocatalytic reactors. I. Optical behaviour of titanium oxide particulate suspensions, J. Photochem. Photobiol. A: Chem. 76 (1993) 199–206.
[32] S. Anandan, M. Yoon, Photocatalytic activities of the nano-sized TiO_2-supported Y-zeolites, J. Photochem. Photobiol. C: Photochem. Rev. 4 (2003) 5–18.